Preparation and properties of novel sulfonated poly(*p*-phenylene-*co*-aryl ether ketone)s for polymer electrolyte fuel cell applications

Xuan Zhang [a], Zhaoxia Hu [a,*], Yanli Pu [b], Shanshan Chen [a], Jiani Ling [a], Huiping Bi [a], Shouwen Chen [a], Lianjun Wang [a,*], Ken-ichi Okamoto [c]

[a] School of Environmental & Biological Engineering, Nanjing University of Science & Technology, Nanjing 210094, China[1]
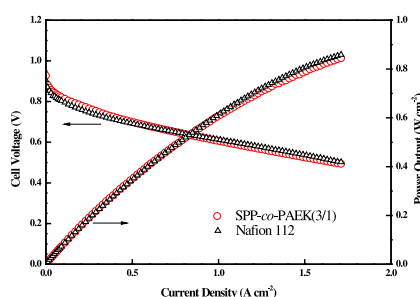[b] Shanxi Applied Physics and Chemistry Research Institute, Xi'an, China
[c] Graduate School of Science & Engineering, Yamaguchi University, Tokiwadai 2-16-1, Ube, Yamaguchi 755-8611, Japan

HIGHLIGHTS

► Sulfonated poly(*p*-phenylene-co-aryl ether ketone) were prepared by Ni(0)-catalyzed copolymerization.
► The anisotropic proton conductivity ratio for the membranes was about 0.85–0.92.
► SPP-co-PAEK(3/1) showed OCV of 0.94 V and output of 0.85 W/cm^2 (90 °C, 82/68 %RH).
► They exhibited good fuel cell performance on a 300 h durability test.

GRAPHICAL ABSTRACT

ABSTRACT

A series of sulfonated poly(*p*-phenylene-*co*-aryl ether ketone) (SPP-*co*-PAEK) membranes are successfully prepared from 2,5-dichloro-3′-sulfobenzophenone and 2,2′-bis[4-(4-chlorobenzoyl)] phenoxyl perfluoropropane through Ni(0)-catalyzed copolymerization for polymer electrolyte membrane fuel cell (PEFC) applications. The obtained SPP-*co*-PAEKs have fairly high reduced viscosities and give ductile and transparent membranes with good mechanical strength. All the membranes exhibit comparable or even better proton conductivities than that of Nafion 112 in the full hydrate state. In addition, the membranes showed almost isotropic proton conductive behavior with $\sigma_\perp/\sigma_\parallel$ values in the range of 0.85–0.92. Fuel cell operation using SPP-*co*-PAEK(3/1) (IEC = 2.0 meq g^{-1}, thickness of 38 μm, feed gases: H$_2$/air) exhibited rather good performances: open circuit voltage of 0.94 V, cell voltage at 1.0 A cm^{-2} of 0.61 V, and output at 1.7 A cm^{-2} of 0.85 W cm^{-2} under 90 °C and 82/68% relative humidity condition. The results suggested that these SPP-*co*-PAEK membranes are promising candidates for PEFC applications.

© 2012 Elsevier B.V. All rights reserved.

1. Introduction

Polymer electrolyte membranes (PEMs) with the "triangle" properties of high performance, good durability and low cost are urgently demanded for the practical PEM fuel cell applications [1–6]. Recently, PEMs based on sulfonated poly(*p*-phenylene)s (SPP) and their derivatives have been the focus of attention of

* Corresponding author. Tel.: +86 25 84315532; fax: +86 25 84315518.
  E-mail addresses: anfanyhu@hotmail.com (Z. Hu), wanglj@mail.njust.edu.cn (L. Wang).
[1] Tel.: +86 25 84315532; fax: +86 25 84315518.

several research groups. This type of polymers could be simply synthesized by Ni(0)-catalyzed coupling copolymerization [7–12]. Their stiff and rod-like chemical structure give them exceptionally good mechanical toughness and chemical stability, which make them quite promising alternatives of the state-of-the-art per-fluorosulfonic acid PEMs (*e.g.* Nafion® of DuPont) [2,5,6,10,13]. McGrath and co-workers prepared poly(*p*-phenylene)s from 2,5-dichloro-4′-substituted benzophenone and several aromatic dichloride compounds and then performed post-sulfonation by fuming or concentrated sulfuric acid [10]. However, these polymers could hardly give tough PEMs and needed to be supported on glass fabrics or via polymer blending strategies. Afterwards, modification of chemical structures such as direct polymerization of sulfonated/ non-sulfonated monomers has been attempted to improve the mechanical properties of this type of PEMs. Zhang and co-workers modified the structure of sulfonated poly(*p*-phenylene)s by intro-ducing dichlorobenzophenone or naphthalimide segments into the polymer backbones [14–17]. Ohira and co-workers prepared a series of sulfonated copoly(*p*-phenylene)s containing alkyl pendants [18,19]. The above developed PEMs had high ion exchange capacity (IEC) levels (above 2.20 meq g^{-1}) and exhibited high proton conductivities as well as other improved performances.

In our previous paper, we developed a series of poly(sulfonated phenylene)-*block*-polyimide copolymers with naphthalimide units in the polymer backbone [20]. The resultant PEMs exhibited distinct hydrophilic-hydrophobic nanophase-separated morphology, largely enhanced hydrolytic stability as well as high proton conductivity. But unfortunately, it was difficult to get high molecular weight copolymers due to the relatively low reactivity and poor solubility of the functional polynaphthalimide oligomers. From the viewpoint of higher reactivity and better solubility, the structure modification of the hydrophobic moieties must be further consid-ered during the polymer structure design.

For the Ni(0)-catalyzed coupling polymerization, the reactivity of the functional aryl chlorides was profoundly influenced by the substituent groups attached to the neighboring phenyl rings. Based on the study of Colon [21] and Bontempelli [22], the aryl chloride with electron-withdrawing substituent groups, such as carbonyl group, nitrile group and acetophenone group, exhibited higher activity and yields. In accordance with the requirement of solubility, the incorporation of ether linkage and/ or perfluoroisopropyl groups in the polymer backbone could largely enhance the solubility. Besides, the presence of hydro-phobic —C(CF$_3$)$_2$— unit might also strengthen the hydrophobicity of the corresponding moieties.

Based on these considerations, we designed a novel non-sulfonated monomer containing ether linkage, perfluoroisopropyl group and carbonyl group *para*- to the aryl chloride groups, named as 2,2′-bis[4-(4-chlorobenzoyl)]phenoxyl perfluoropropane (BCPPF), for the preparation of novel sulfonated poly(*p*-phenylene)s. This monomer could be readily synthesized via a Friedel–Crafts acylation and nucleophilic substitution reaction. Through Ni(0)-catalyzed coupling copolymerization with the sulfonated mono-mer of 2,5-dichloro-3′-sulfobenzophenone (DCSB), a series of sulfonated poly(*p*-phenylene-*co*-aryl ether ketone)s (SPP-*co*-PAEKs) had been successfully developed. We have attempted to prepare blend membranes with sulfonated polyimide (SPI) and gained valuable results, especially of that the proton conductivity anisotropy ($\sigma_\perp/\sigma_\parallel$) was largely suppressed compared with the pristine SPI PEMs [23]. Therefore, it is quite interesting to investi-gate the properties of SPP-*co*-PAEKs themselves in details. Herein, we report the detailed properties of PEMs derived from SPP-*co*-PAEKs including IEC, water uptake (WU), size change, mechanical properties, proton conductivity, fuel cell performance and durability.

2. Experimental

2.1. Materials

2,5-Dichlorobenzoic acid (Wuhan Fuchi Biological Technology Chemical, China), benzene (GuangDong Guanghua Chemical Factory, China), fluorobenzene (Zhejiang Rainful Chemical, China), *p*-chlorobenzoyl chloride (Jintan Lanling Chemicals, China), 4,4′-(hexafluoroisopropylidene) diphenol (Zhejiang Norchain Tech-nology Development Co., Ltd, China) and fuming sulfuric acid (SO$_3$, 50%) (Shanghai Zhenhua Chemical, China) were used as received. 2,5-Dichlorobenzophenone was prepared by AlCl$_3$ catalytic Friedel–Crafts acylation of 2,5-dichlorobenzoyl chloride with benzene and recrystallized from ethanol (yield: 90%) [23]. Reagent-grade anhydrous NiBr$_2$ was purchased from Aldrich and dried at 200 °C under vacuum. Triphenylphosphine (PPh$_3$) was purchased from Aldrich and recrystallized from hexane prior to use. N,N′-Dimethylacetamide (DMAc) was dried over CaH$_2$, distilled under reduced pressure and stored over 4 Å molecular sieves prior to use. Zinc dust (Sinopharm Chemical Reagent Corporation, China) was stirred with 2 M HCl for 5 min, filtrated, then washed thoroughly with distilled-water, ethanol, ethyl ether, successively, and dried under vacuum. Nafion solution (5 wt%) was purchased from Wako and used as received. Pt/C electrodes (#45372) were purchased from Johnson Matthey Plc.. All other chemicals were used as received.

2.2. Synthesis of monomers

DCSB and BCPPF were synthesized according to the literature [23]. DCSB: ^{1}H NMR (D$_2$O): 8.07–8.12 ppm (s, 1H), 7.93–8.00 ppm (d, 1H), 7.67–7.75 ppm (d, 1H), 7.43–7.52 ppm (t, 1H), 7.30–7.42 ppm (m, 3H). BCPPF: ^{1}H NMR (CDCl$_3$): 7.79–7.84 (d, 1H), 7.71–7.76 (d, 1H), 7.42–7.48 (m, 2H), 7.05–7.19 (m, 2H).

2.3. Synthesis of SPP-co-PAEK copolymers

In this study, the nomenclature of the SPP-*co*-PAEK copolymers is SPP-*co*-PAEK(x/y), where the data in the parenthesis refer to the molar ratio of DCSB to BCPPF. A typical synthesis procedure of SPP-*co*-PAEK(2/1) was performed as follows.

To a 50 mL three-necked flask, which was equipped with a nitrogen inlet/outlet, were charged with 0.138 g of anhydrous NiBr$_2$ (0.63 mmol), 1.157 g of PPh$_3$ (4.41 mmol) and 2.332 g of zinc dust (35.66 mmol). After being evacuated and filled with nitrogen three times, 6.0 mL of DMAc was added. The mixture was stirred at 80 °C until the color changed to reddish-brown (about 20 min), then 10.0 mL of DMAc solution containing 2.119 g of DCSB (6.00 mmol) and 2.297 g of BCPPF (3.00 mmol) was added into the flask. The reaction was performed at 80 °C for 8 h. The resulting viscous mixture was poured into 300 mL of 10% HCl solution. The fiber-like polymer was collected by filtration, dried under vacuum, dissolved in 10 wt% of DMAc and then re-precipitated in isopropanol. After filtration, the white solid was dried under vacuum (yield: 95%).

2.4. Membrane preparation and acidification

The SPP-*co*-PAEK membranes were prepared by solution casting method. Firstly, SPP-*co*-PAEK solutions in DMAc (7% w/v) were filtrated and cast onto a clean Petri dish and dried at 80 °C for 24 h. Secondly, the membranes were detached by immersing into distilled water, followed by proton exchange in 2 M HCl at 50 °C for 72 h. Finally, the membranes were thoroughly washed with de-ionized water, fixed in a stainless frame and dried under vacuum at 120 °C for 2 h. The thickness of the membranes was controlled to be about 40 μm.

2.5. Characterization

2.5.1. Measurements

^{1}H NMR spectra were performed on a Bruker spectrometer (300 MHz, Switzerland). Mechanical property of the SPP-co-PAEK membranes was analyzed by tensile measurement, which was performed with a universal testing instrument (Shimadzu, AGS-X 349-05489A) at 20 °C and around 50% relative humidity (RH) at a crosshead speed of 2 mm min^{-1}.

2.5.2. Water uptake, size change and IEC

Water uptake, size change and IECs were measured according to the method described elsewhere [24–26]. The membranes were dried at 120 °C under vacuum for 2 h to get the dry weight (W_d), and then immersed in de-ionized water at 30 °C for 5 h to get the wet weight (W_w). The water uptake of the membranes was calculated from Eq. (1):

$$WU(\%) = (W_W - W_d)/W_d \times 100\% \qquad (1)$$

For size change measurements, circular membrane sheets were soaked into de-ionized water at 30 °C for 5 h the size change in the membrane thickness direction (Δt_c) and the plane direction (Δl_c) were calculated from Eq. (2):

$$\Delta t_c = (t - t_s)/t_s \\ \Delta l_c = (l - l_s)/l_s \qquad (2)$$

where t_s and l_s refer to the thickness and diameter of the membrane equilibrated at 70% RH, respectively; t and l refer to those of the membrane immersed in water.

IECs of the membranes were determined by a titration method. The proton-type samples were ion-exchanged by a 15 wt% NaCl solutions and titrated with a 0.02 M NaOH solution with phenolphthalein as the indicator. IEC was calculated from Eq. (3):

$$IEC = C_{NaOH} \times V_{NaOH}/W_d \qquad (3)$$

where C_{NaOH} and V_{NaOH} are the concentration of NaOH solution and the consumed volume of NaOH solution, respectively.

2.5.3. Proton conductivity

In-plane ($\sigma_\parallel$) and through-plane proton conductivity ($\sigma_\perp$) were determined using an electrochemical impedance spectroscopy technique over the frequency of 0.01–100 kHz (Hioki 3532-50). For $\sigma_\parallel$, a single cell with two platinum plate electrodes was mounted on a Teflon plate at 1.5 cm distance. For $\sigma_\perp$, a membrane sample was set between two platinum plate electrodes of 1.0 cm^2 area, and mounted on two Teflon blocks. The cells were placed in a thermo-controlled humidified vessel or in liquid water. Proton conductivity ($\sigma_\parallel$ and $\sigma_\perp$) and anisotropic proton conductivity ratio ($\sigma_{\perp/\parallel}$) were calculated from Eq. (4):

$$\sigma_\parallel = d/(\omega_s t_s R) \\ \sigma_\perp = t_s/(AR) \\ \sigma_{\perp/\parallel} = \sigma_\perp/\sigma_\parallel \qquad (4)$$

where d is the distance between two electrodes, t_s and ω_s are the thickness and width of the membrane at 70% RH, respectively, A is the electrode area and R is the resistance value measured. As for the measurements in liquid water, the swollen membrane thickness was used.

2.5.4. Fabrication of membrane electrode assembly (MEA) and measurements of fuel cell performance

An MEA was fabricated from a membrane sample (2.5 × 2.5 cm) by hot-pressing an electrode/membrane/electrode sandwich at 150 °C for 5 min under 5.88 MPa. Prior to the hot-pressing, both surfaces of the membrane and Pt/C electrodes were impregnated with Nafion solution (5 wt%) as a binder. The effective electrode area was 5 cm^2. The MEA was set in a single cell test fixture and mounted into an in-house fuel cell test station (NF Inc., model As-510), which was supplied with temperature-controlled humidified gases.

The PEM fuel cell performance was evaluated at cell temperatures of 90 °C, back pressures of 0.2 MPa and different gas humidification temperatures of 85/80 °C, 72/72 °C and 59/59 °C for anode/cathode gases, respectively. The gas flow was controlled to keep the utilization of H$_2$ (anode) constant at 60, 70 or 80% and of air (cathode) constant at 15, 32 or 50%, corresponding to the gas humidification temperature of 85/80 °C, 72/72 °C and 59/59 °C, respectively. The cell resistance (R_c) and electrode reaction resistance (R_{el}) were determined from the AC impedance cole–cole plots. The through-plane proton conductivity under fuel cell operation ($\sigma_{\perp,FC}$) was evaluated by assuming that the membrane resistance is approximately equal to the cell resistance.

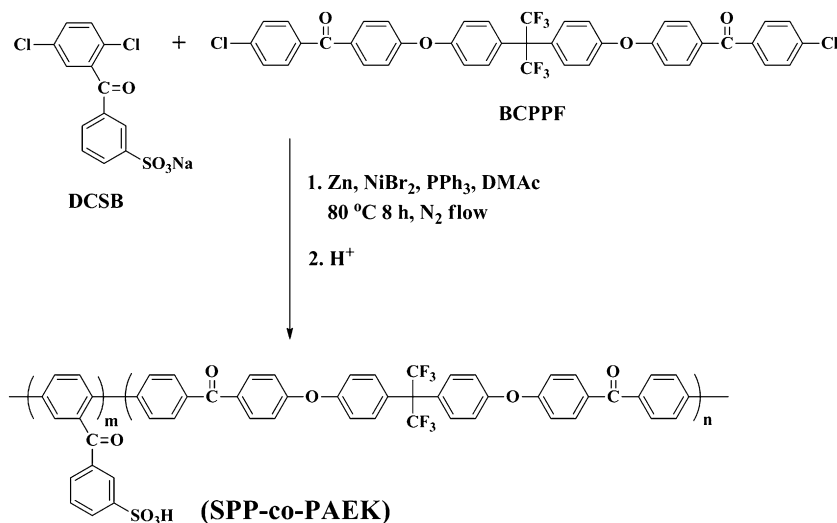## 3. Results and discussion

3.1. Synthesis and characterization

Monomer named as BCPPF with perfluoroisopropyl group and carbonyl group para- to the aryl chloride groups was synthesized and functioned as the hydrophobic moieties in the polymer backbone. As illustrated in Scheme 1, the Ni(0)-catalyzed coupling polymerization proceeded homogenously in DMAc to produce SPP-co-PAEK copolymers with reduced viscosity values of 0.42–0.71 dL g^{-1}, indicating their fairly high molecular weight as noted in Table 1. The chemical structures of the copolymers were confirmed by ^{1}H NMR. All the peaks were well assigned to the protons as designated in Fig. 1. Fig. S1 showed the H–H COSY spectrum of SPP-co-PAEK(3/1)(see Supporting information). All the obtained copolymers showed excellent solubility in polar organic solvents and formed transparent and ductile films by solution casting method.

3.2. Mechanical properties

Typical tensile stress–strain curves and the representative data (M, S, E_b) of all the SPP-co-PAEK membranes were shown in Fig. 2 and Table 1. They exhibited reasonably high mechanical strength with Young's modulus (M), maximum stress (S) and elongation at break (E_b) values ranged from 1.3 to 1.8 GPa, 46–54 MPa and 34–73%, respectively. As clearly shown in Fig. 2, all the SPP-co-PAEK membranes displayed distinct yield point at the elongation degree around 5%. It suggested that the membranes could undergo fairly large deformation or sustain quite high external impact without break in practical applications, especially in the process of MEA preparation. In addition, with the increasing of the content of rigid phenylene moieties in the copolymer backbone, Young's modulus of the corresponding membrane reached a maximum of 1.8 GPa for the membrane of SPP-co-PAEK(3/1). This might indicate that appropriate level of rigidity of the polymer backbone is favorable to improve mechanical strength for this type of PEMs.

3.3. IEC, size change, WU and proton conductivity

Table 1 lists the IEC, WU, size change data of the SPP-co-PAEK membranes together with Nafion 112 for comparison. For all the SPP-co-PAEK membranes in this study, the IECs were readily controlled from 1.65 to 2.51 by adjusting the feed ratio of DCSB to BCPPF from 2/1 to 5/1.

Scheme 1. The synthetic route for SPP-*co*-PAEK copolymer in proton form.

As well-known, water uptake and size change of a PEM have profound effect on membrane conductivity and mechanical properties. Water molecules usually facilitate proton transfer, however, excessive water uptakes inevitably lead to the undesirable membrane swelling, which might cause damage to the MEA integrity [27,28]. It is apparent that WUs of the present PEMs increased with the increase in IEC values, as listed in Table 1. The hydration number (λ) values were in the range of 11–15, which were about two thirds of that of Nafion 112. Comparing with other two types of SPPs (I-70 and BC5) as shown in Table 1, the SPP-*co*-PAEK membranes displayed almost isotropic membrane swelling with slightly larger size change in the thickness direction, while I-70 and BC5 showed distinct anisotropic behavior. For example, the membrane of SPP-*co*-PAEK(3/1) showed size change of 0.12 and 0.13 in plane and thickness direction, respectively, whereas 0.07 and 0.45 for I-70 as well as 0.11 and 0.31 for BC5. The difference in their hydrophobic moieties brought out the difference in the swelling behavior greatly. The coplanar naphthalimide architecture and strong inter-chain interaction would cause the alignment of the polymer backbone in plane direction during the formation of membrane [29]. While in the case of the present membranes, the polymer molecules might tend to arrange randomly due to their much weaker inter-chain interactions, thus they exhibited the isotropic swelling behavior after absorbing water.

Fig. 3 shows the *in-plane* proton conductivities ($\sigma_{||}$) of SPP-co-PAEK membranes as a function of relative humidity at 60 °C, Fig. 4 shows their temperature dependence in water at 20–90 °C. Table 1 also lists the $\sigma_{||}$ data at 50%, 70% RH and in liquid water. The proton conductivities were closely related to their IECs and RHs for all the present SPP-*co*-PAEK membranes. For example, the membrane of SPP-*co*-PAEK(2/1) (1.65 meq g^{-1}) displayed $\sigma_{||}$ of 93 mS cm^{-1} in water at 60 °C, whereas the data significantly increased to 223 mS cm^{-1} for SPP-*co*-PAEK(5/1) with the IEC of 2.51 meq g^{-1}. In water, the membrane with IEC over 2.0 meq g^{-1} exhibited higher $\sigma_{||}$ values than Nafion at 30–90 °C. The activation energy was in the range of 14–16 kJ mol^{-1}, which was slightly larger than that of Nafion (12 kJ mol^{-1}). On the other hand, this type of PEMs showed larger RH dependence. For example, the SPP-*co*-PAEK(5/1) membrane exhibited $\sigma_{||}$ value of 1.7 mS cm^{-1} at 30% RH, which was only about a third to that of Nafion 112. However, it increased to 92 and 223 mS cm^{-1} at 80% RH and full hydrated condition, respectively. Similar phenomena have been reported by almost all the hydrocarbon-type ionomers ascribing to the stronger acidity for the sulfonic acid groups of Nafion, its unique ion-cluster morphology together with the high volumetric IEC (2.1 meq cm^{-3}) [20,23–27,30]. While comparing SPP-*co*-PAEK(3/1) to BC5 (see Table 1) with the similar titrated IEC values, the former exhibited slightly lower $\sigma_{||}$ values under partial hydrated conditions. This

Table 1
Physical properties of SPP-*co*-PAEK membranes and Nafion 112.

Ionomer	IEC[a]	η_r[b]	WU[c]	Size Change[c]		$\sigma_{||}$(mS cm^{-1})[d]			$\sigma_\perp$	$\sigma_\perp/\sigma_{||}$	Strain-Stress		
	meq g^{-1}	dL g^{-1}	%	Δt_c	Δl_c	50%	70%	In water			M(GPa)	E(%)	S(MPa)
SPP-*co*-PAEK(2/1)	1.65(1.42)	0.42	34	0.08	0.07	4.8	24.1	93	82	0.88	1.4	43	54
SPP-*co*-PAEK(2.5/1)	1.86(1.71)	0.50	40	0.10	0.10	6.5	25.1	127	108	0.85	1.5	34	49
SPP-*co*-PAEK(3/1)[e]	2.03(1.98)	0.71	55	0.13	0.12	7.4	33.3	164	148	0.90	1.8	63	51
SPP-*co*-PAEK(4/1)	2.30(2.20)	0.49	59	0.15	0.13	12.1	38.9	177	159	0.90	1.6	65	51
SPP-*co*-PAEK(5/1)	2.51(2.38)	0.67	70	0.19	0.17	10.3	44.7	223	205	0.92	1.3	73	46
I-70[f]	2.47(2.41)	–	118	0.45	0.07	–	–	–	–	–	–	–	–
BC5[g]	2.50(1.92)	–	73	0.31	0.11	11	36	203	176	0.87	–	–	–
Nafion 112	0.91(0.89)	–	35	0.11	0.11	15.8	46.5	143	139	0.97	0.2	410	37

[a] Calculated data and experimental data in parentheses.
[b] Reduced viscosity measured at 0.5 g dL^{-1} in NMP(1% LiCl) at 35 °C.
[c] At 30 °C.
[d] At 60 °C.
[e] Cited from [23].
[f] Prepared from DCSB and bis(N-(4-chloro-2-trifluoromethylphenyl)-1,4,5,8-naphthalimide), cited from [14].
[g] Prepared from DCSB and dichloro(polynaphtalimide) oligomer, cited from [20].
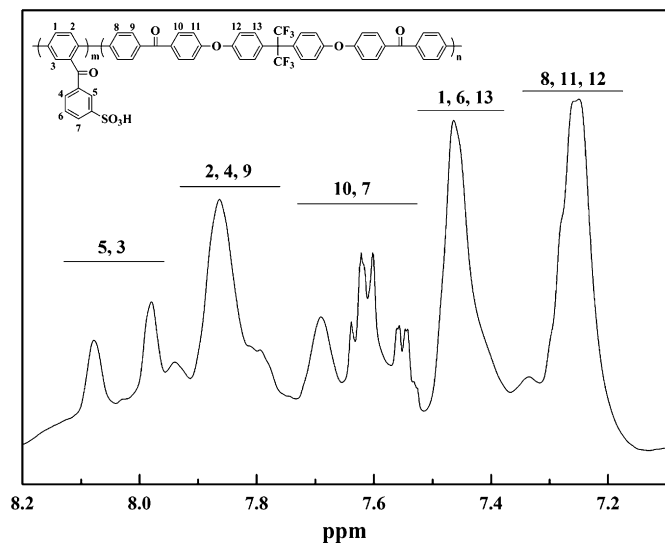
Fig. 1. ^{1}H NMR spectra of SPP-*co*-PAEK(3/1) in DMSO-d_6 at 25 °C.

Fig. 3. Proton conductivity of SPP-*co*-PAEK membranes as a function of relative humidity.

3.4. PEFC performance

As discussed above, the membrane of SPP-*co*-PAEK(3/1) showed good mechanical property, similar size change and comparable proton conductivity in both directions to Nafion 112. Therefore, MEA was fabricated from this membrane and fuel cell performance was carried out with supply of hydrogen/air as the anode/cathode feed gas under 0.2 MPa at 90 °C. The polarization curves were obtained with the gas humidification temperatures set at 85/80 °C, 72/72 °C and 59/59 °C for anode/cathode, which were corresponded to 82/68% RH, 48/48% and 27/27% RH (abbreviated to 82/68%, 48% and 27% RH afterwards), respectively, and shown in Fig. 6(a)–(c).

At a humidification temperature of 85/80 °C, the SPP-*co*-PAEK(3/1) showed the high PEM fuel cell performance. For example, open circuit voltage (OCV) of 0.94 V, cell voltage at current density of 1.0 A cm^{-2} ($V_{1.0}$) of 0.61 V, and output at 1.7 A cm^{-2} of 0.85 W cm^{-2}. These primary results indicated the integrity of the prepared MEA and normal function of the catalyst electrodes. It displayed almost the same curve to that of Nafion 112 under the similar condition (OCV of 0.93 V, $V_{1.0}$ of 0.61 V, and output at 1.7 A cm^{-2} of 0.86 W cm^{-2}). With decreasing the relative humidity from 82/68% RH to 48/48% RH and then to 27/27% RH, the cell performance

could be explained by the existence of distinct hydrophilic-hydrophobic microphase-separation morphology in the latter. In practical cell operation, the proton conductivity in the thickness direction is more concerned. As for this type of PEMs, the $\sigma_\perp$ values measured in water at 60 °C also depended on the IECs greatly, which were comparable to that in the plane direction, 85–92% as noted in Table 1. Under partial hydrated state, it is reasonable to predict that they will show similar tendency.

Fig. 5 shows the relationships of relative WU and volume change (ΔV_{olu}) versus relative proton conductivity. Clearly, the SPP-*co*-PAEK membranes displayed a larger WU curve than that of Nafion, which suggested the former needed more water absorption to reach to the same level of proton conductivity than the latter. On the other hand, relative ΔV_{olu} of SPP-*co*-PAEK(2.5/1) and SPP-*co*-PAEK(3/1) were close to the state of Nafion 112. Since they were isotropic in swelling state, these results might reveal the similar internal relationship between swelling and proton conductive behavior for SPP-co-PAEKs and Nafion. As for comparison, the membranes of BC5 needed much more water molecules to produce the comparable proton conductivity, resulting in the larger swelling state inevitably.
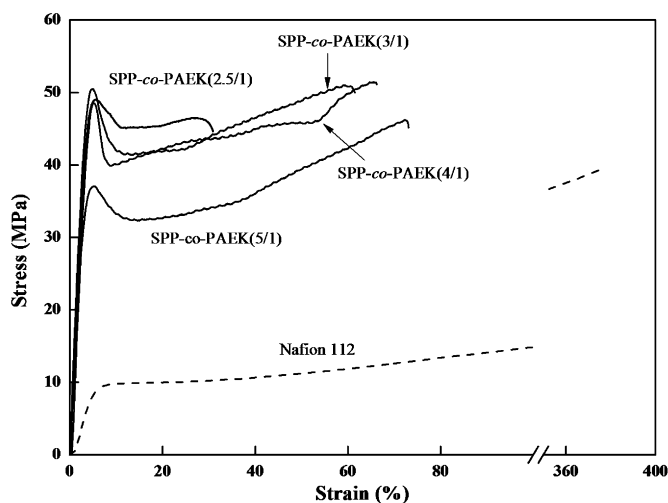

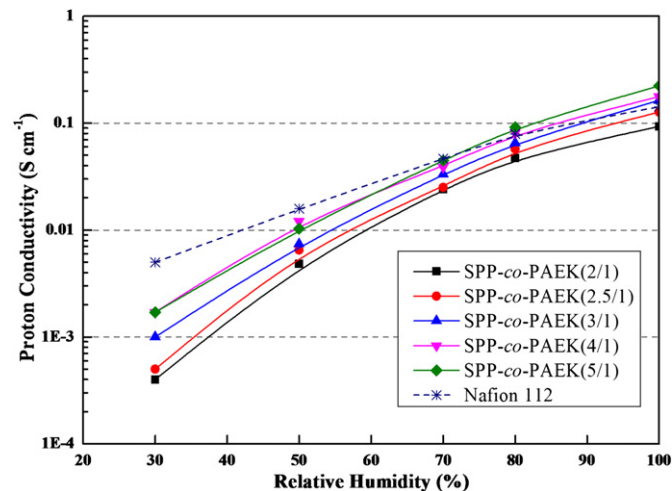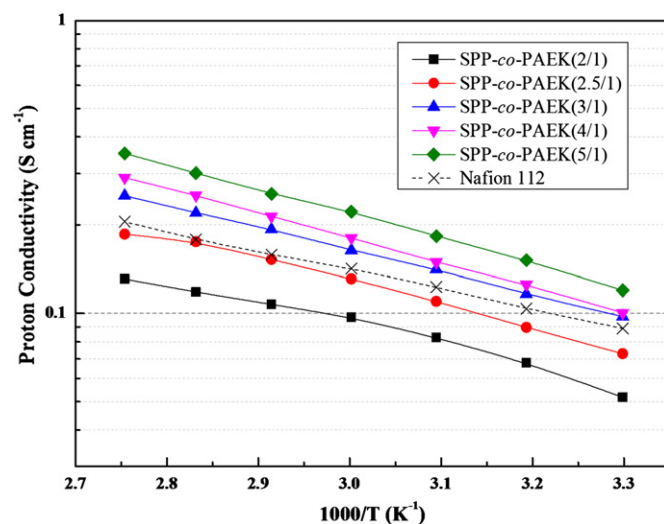**Fig. 2.** Stress-Strain curves of SPP-*co*-PAEKs and Nafion 112.

Fig. 4. Proton conductivity of SPP-*co*-PAEK membranes as a function of temperature.
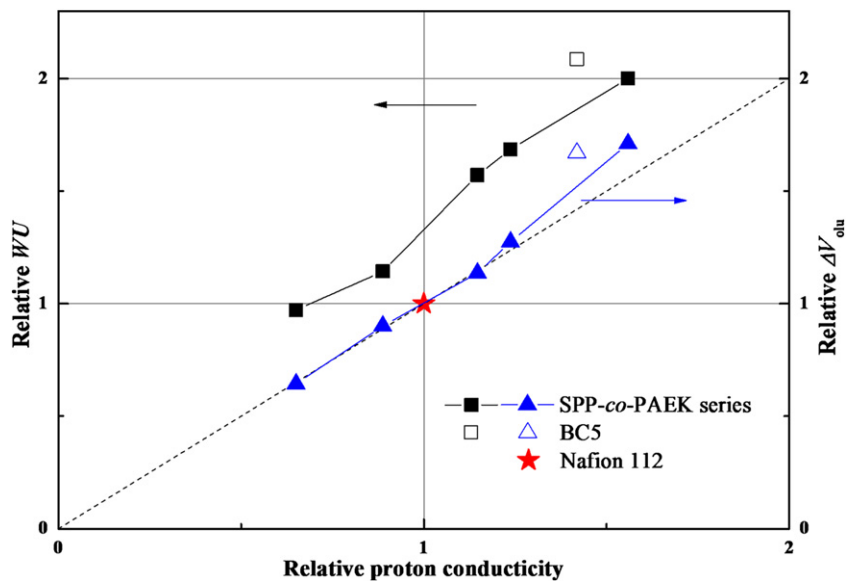
Fig. 5. The relationship of WU, ΔV_{olu} and proton conductivity of SPP-*co*-PAEKs and BC5 based on Nafion 112 as a benchmark.
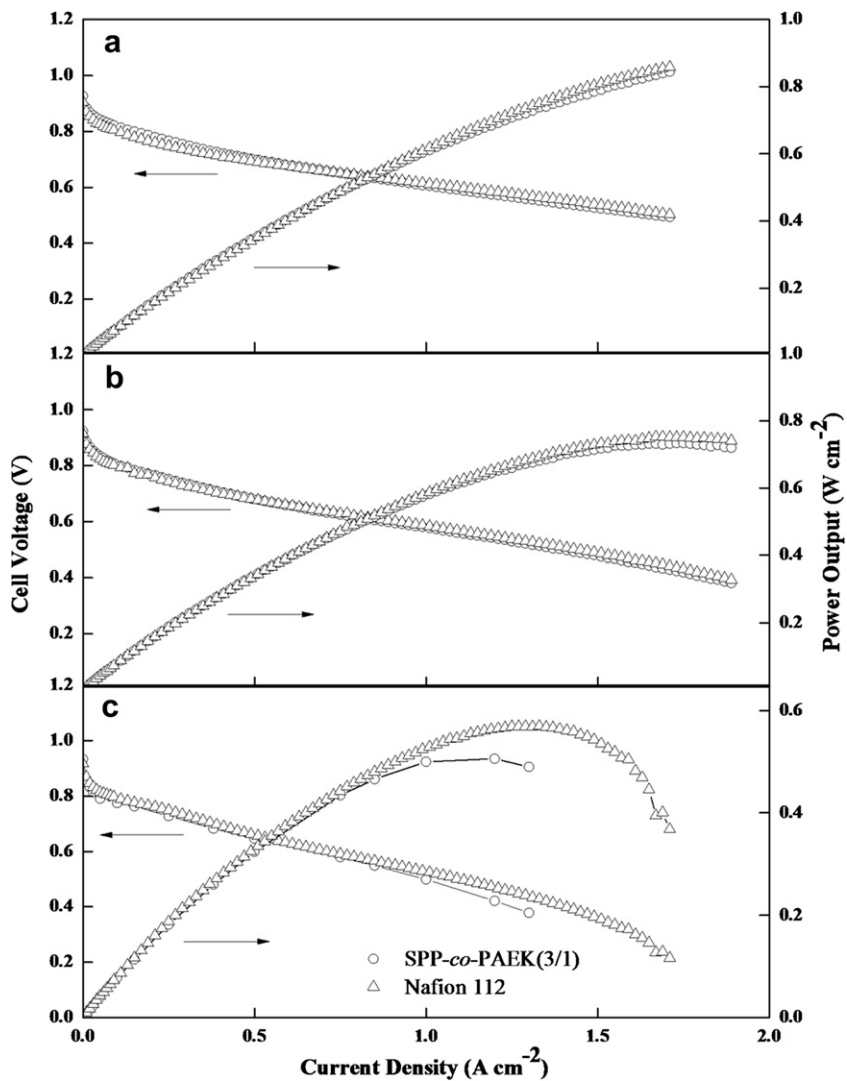

Fig. 6. Performance of PEFCs with SPP-*co*-PAEK(3/1) and Nafion 112 at 90 °C/0.2 MPa with supply of (a) H_2/air (60% H_2/15% air) and gas humidification temperature of 85/80 °C, (b) H_2/air (70% H_2/32% air) and gas humidification temperature of 72/72 °C and (c) H_2/air (80% H_2/50% air) and gas humidification temperature of 59/59 °C.

decreased slightly, as shown in Fig. 6(b) and Fig. 6(c). For example, OCV of 0.95 V, $V_{1.0}$ of 0.58 V, W_{max} of 0.73 W cm^{-2} for 48/48% RH and OCV of 0.93 V, $V_{1.0}$ of 0.50 V, W_{max} of 0.51 W cm^{-2} for 27/27% RH. These performances were still kept at the relative high level and were comparable to Nafion 112 but much higher than some SPIs as reported [31,32].

By assuming that the membrane resistance equal to R_c, the *through-plane* proton conductivity ($\sigma_{\perp,FC}$) under PEFC operation was evaluated and noted to reflect the behavior of the cell performance well as mentioned above. The $\sigma_{\perp,FC}$ values for SPP-*co*-PAEK(3/1) were 54, 37 and 27 mS cm^{-1} under 82/68%, 48/48% and 27/27% RH at 1 A cm^{-2}, respectively. These relatively large $\sigma_{\perp,FC}$ values were responsible for the relatively high cell performance under whole humidification range from 82/68% to 27/27% RH. The *in-plane* proton conductivity ($\sigma_{\parallel}$) at 80% RH and 60 °C was 65 mS cm^{-1} (See Fig. 3). Assuming the activation energy of $\sigma_{\parallel}$ as 15 kJ mol^{-1} and the anisotropy ratio of proton conductivities ($\sigma_{\perp}/\sigma_{\parallel}$) as 0.90, the $\sigma_{\perp}$ value was estimated to be about 91 mS cm^{-1} under 80% RH at 90 °C, which was rather higher than the measured value of 54 mS cm^{-1}. A possible explanation might be that the real hydrated state is below 80% for the membrane, another one might be attributed to the contact resistance of membrane/electrode interfaces.

As for the durability test, a PEFC with SPP-*co*-PAEK(5/1) was operated for 311 h under the conditions of a constant current density of 0.2 A cm^{-2}, cell temperature of 90 °C and feed gas of 0.2 MPa under 48/48% RH. The OCV, cell voltage and cell resistance were monitored during the test. During the durability test, the polarization curves and impedance spectra were measured several times. The results are shown in Fig. 7 and listed in Table 2. The OCV, cell resistance and cell voltage ($V_{0.2}$) were constant at 0.93 V, 20 mΩ and 0.71 V during the durability test, respectively. Generally, OCV is strongly influenced by the fuel permeability across the membrane as well as the reactant concentrations. The constant OCV during the durability test indicated the normal function of the MEA as well as the stability of the SPP-*co*-PAEK membrane during the test [33]. No remarkable reduction in the cell performance was observed during the operation. However, a slight drop in the membrane proton conductivity in the thickness direction was also found, which was explainable for the change in the cell performance. The lower content of water absorbed in the membrane under low RH of 50% and the insufficient water back diffusion from cathode to anode during the operation might be one reason causing the drop in proton conductivity.
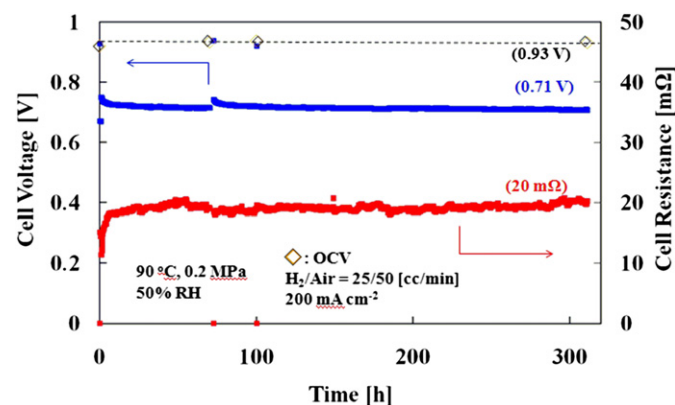
Table 2
PEFC durability test data for SPP-*co*-PAEK(5/1).

Elapsed time (h)	OCV (V)	W_{max} (W cm^{-2})	$V_{0.5}$ (V)	$\sigma_{\perp}(V_{0.5})$ (mS cm^{-1})	$V_{1.0}$ (V)	$\sigma_{\perp}(V_{1.0})$ (mS cm^{-1})	$V_{1.5}$ (V)	$\sigma_{\perp}(V_{1.5})$ (mS cm^{-1})
0 h	0.93	0.63	0.63	50	0.52	59	0.42	60
311 h	0.93	0.59	0.61	48	0.50	53	0.40	54

4. Conclusion

A series of SPP-co-PAEK copolymers were successfully prepared from DCSB and BCPPF (molar ratio: 2:1–5:1) through Ni(0)-catalyzed copolymerization, and subsequently used to prepare PEMs by solution casting method. It gave transparent membranes which exhibited good mechanical strength and isotropic swelling behavior in water. The *in-plane* and *through-plane* proton conductivities of SPP-*co*-PAEK membranes were 93–223 and 82–205 mS cm^{-1} at 60 °C in water, respectively, and the anisotropic proton conductivity ratio was about 0.85–0.92. The membrane of SPP-*co*-PAEK(3/1) with IEC of 2.0 meq g^{-1} showed high PEFC performance of open circuit voltage (OCV) of 0.94 V, cell voltage at current density of 1.0 A cm^{-2} ($V_{1.0}$) of 0.61 V, and output at 1.7 A cm^{-2} of 0.85 W cm^{-2} under 90 °C, 82/68% RH condition (H$_2$/air). Hardly reduction in the cell performance was observed during the short term durability test for the membrane of SPP-*co*-PAEK(5/1). Those results indicated the good potentials of this type of membranes for PEFC applications.

Acknowledgments

Appendix A. Supplementary material

Supplementary data associated with this article can be found, in the online version, at doi:10.1016/j.jpowsour.2012.05.016.

References

[1] J.A. Kerres, J. Membr. Sci. 185 (2001) 3–27.
[2] M. Rikukawa, K. Sanui, Prog. Polym. Sci. 25 (2000) 1463–1502.
[3] M.A. Hickner, Mater. Today 13 (2010) 34–41.
[4] T.J. Peckham, S. Holdcroft, Adv. Mater. 22 (2010) 4667–4690.
[5] K.A. Mauritz, R.B. Moore, Chem. Rev. 104 (2004) 4535–4585.
[6] M.A. Hickner, H. Ghassemi, Y.S. Kim, B.R. Einsla, J.E. McGrath, Chem. Rev. 104 (2004) 4587–4612.
[7] B.M. Rosen, K.W. Quasdorf, D.A. Wilson, N. Zhang, A.-M. Resmerita, N.K. Garg, V. Percec, Chem. Rev. 111 (2011) 1346–1416.
[8] K. Goto, I. Rozhanskii, Y. Yamakawa, T. Otsuki, Y. Naito, Polym. J. 41 (2009) 95–104.
[9] M. Ueda, F. Ichikawa, Macromolecules 23 (1990) 926–930.
[10] H. Ghassemi, J.E. McGrath, Polymer 45 (2004) 5847–5854.
[11] C.H. Fujimoto, M.A. Hickner, C.J. Cornelius, D.A. Loy, Macromolecules 38 (2005) 5010–5016.
[12] G. Maier, J.M. -Haack, Adv. Polym. Sci. 216 (2008) 1–62.
[13] T. Kobayashi, M. Rikukawa, K. Sanui, N. Ogata, Solid State Ionics 106 (1998) 219–225.
[14] Z. Qiu, S. Wu, Z. Li, S. Zhang, W. Xing, C. Liu, Macromolecules 39 (2006) 6425–6432.
[15] F. Zhang, Z. Cui, N. Li, L. Dai, S. Zhang, Polymer 49 (2008) 3272–3278.
[16] W. Li, Z. Cui, X. Zhou, S. Zhang, L. Dai, W. Xing, J. Membr. Sci. 315 (2008) 172–179.
[17] S. Wu, Z. Qiu, S. Zhang, X. Yang, F. Yang, Z. Li, Polymer 47 (2006) 6993–7000.
[18] S. Seesukphronrarak, K. Ohira, K. Kidena, N. Takimoto, C.S. Kuroda, A. Ohira, Polymer 51 (2010) 623–631.
[19] S. Seesukphronrarak, A. Ohira, Chem. Commun. 47 (2009) 4744–4746.

Fig. 7. Variation of OCV and cell resistance of PEFCs with SPP-co-PAEK(5/1) during the short durability test.

[20] H. Bi, S. Chen, X. Chen, K. Chen, M. Higa, N. Endo, K. Okamoto, L. Wang, Macromol. Rapid Commun. 30 (2009) 1852–1856.
[21] I. Colon, D.R. Kelsey, J. Org. Chem. 51 (1986) 2627–2637.
[22] G. Schiavon, G. Bontempelli, B. Corain, J. Chem. Soc. Dalton Trans. 5 (1981) 1074–1081.
[23] X. Zhang, S. Chen, J. Liu, Z. Hu, S. Chen, L. Wang, J. Membr. Sci. 371 (2011) 276–285.
[24] X. Zhang, Z. Hu, S. Zhang, S. Chen, S. Chen, J. Liu, L. Wang, J. Appl. Polym. Sci. 121 (2011) 1707–1716.
[25] S. Chen, Y. Yin, K. Tanaka, H. Kita, K.-i. Okamoto, Polymer 47 (2006) 2660–2669.
[26] X. Zhang, Z. Hu, L. Luo, S. Chen, J. Liu, S. Chen, L. Wang, Macromol. Rapid Commun. 32 (2011) 1108–1113.
[27] B. Bae, T. Yoda, K. Miyatake, H. Uchida, M. Watanabe, Angew. Chem. Int. Ed. 49 (2010) 317–320.
[28] Z. Hu, Y. Yin, S. Chen, O. Yamada, K. Tanaka, H. Kita, K.-i. Okamoto, J. Polym. Sci. Part A: Polym. Chem. 44 (2006) 2862–2872.
[29] Z. Hu, Y. Yin, K. Yaguchi, N. Endo, M. Higa, K-i. Okamoto, Polymer 50 (2009) 2933–2943.
[30] C.A. Edmondson, J.J. Fontanella, Solid State Ionics 152-153 (2002) 355–361.
[31] K. Okamoto, K. Yaguchi, H. Yamamoto, K. Chen, N. Endo, M. Higa, H. Kita, J. Power Sources 195 (2010) 5856–5861.
[32] K. Yaguchi, K. Chen, N. Endo, M. Higa, K.-i. Okamoto, J. Power Sources 195 (2010) 4676–4684.
[33] EG&G Technical Services, Inc., Fuel Cell Handbook, seventh ed., U.S. DOE, National Energy Technology Laboratory, Office of Fossil Energy, Morgantown, 2004.